

This is an Open Access document downloaded from ORCA, Cardiff University's institutional repository: <https://orca.cardiff.ac.uk/id/eprint/137859/>

This is the author's version of a work that was submitted to / accepted for publication.

Citation for final published version:

Durand, Eliot , Lobo, Prem, Crayford, Andrew , Sevcenco, Yura and Christie, Simon  
2021. Impact of fuel hydrogen content on non-volatile particulate matter emitted from an aircraft auxiliary power unit measured with standardised reference systems. Fuel 287 , 119637. 10.1016/j.fuel.2020.119637

Publishers page: <http://dx.doi.org/10.1016/j.fuel.2020.119637>

Please note:

Changes made as a result of publishing processes such as copy-editing, formatting and page numbers may not be reflected in this version. For the definitive version of this publication, please refer to the published source. You are advised to consult the publisher's version if you wish to cite this paper.

This version is being made available in accordance with publisher policies. See <http://orca.cf.ac.uk/policies.html> for usage policies. Copyright and moral rights for publications made available in ORCA are retained by the copyright holders.



1 **Impact of fuel hydrogen content on non-volatile particulate**  
2 **matter emitted from an aircraft auxiliary power unit**  
3 **measured with standardised reference systems**

4  
5 Eliot Durand <sup>a\*</sup>, Prem Lobo <sup>b</sup>, Andrew Crayford <sup>a</sup>, Yura Sevcenco <sup>a</sup>, Simon Christie <sup>c</sup>

6  
7 <sup>a</sup> Gas Turbine Research Centre, Cardiff University, Cardiff, United Kingdom

8 <sup>b</sup> Metrology Research Centre, National Research Council Canada, Ottawa, Ontario, Canada

9 <sup>c</sup> Centre for Aviation, Transport and the Environment, Manchester Metropolitan  
10 University, Manchester, United Kingdom

11  
12  
13  
14  
15  
16  
17  
18  
19  
20  
21  
22  
23  
24  
25

---

\* Corresponding authors

E-mail address: [DurandEF@cardiff.ac.uk](mailto:DurandEF@cardiff.ac.uk), Prem.Lobo@nrc-cnrc.gc.ca

Postal address: Cardiff School of Engineering, Queen's buildings, 14-17 The Parade, Cardiff, CF24 3AA, United Kingdom

26  
27  
28  
29  
30  
31  
32  
33  
34  
35  
36  
37  
38  
39  
40  
41  
42  
43  
44  
45  
46  
47  
48

## Highlights

- Increasing fuel hydrogen content systematically reduced nvPM number, mass, and size
- Measured nvPM emissions were loss corrected using particle size distributions
- Particle loss correction factors are impacted by fuel composition and APU condition
- APU exit nvPM emissions were inversely correlated with fuel hydrogen content

49        **Abstract**

50        Replacement of conventional petroleum jet fuel with sustainable aviation fuels (SAFs) can significantly  
51        reduce non-volatile Particulate Matter (nvPM) emissions from aircraft main engines and auxiliary  
52        power units (APUs). As part of the Initiative Towards sustAinable Kerosene for Aviation (ITAKA)  
53        project, the impact of fuel hydrogen content on nvPM number and mass emissions and particle size  
54        distributions were investigated using a GTCP85 APU burning blends of conventional (Jet A-1) and  
55        Hydrotreated Esters and Fatty Acids (HEFA)-derived (Used Cooking Oil and Camelina) aviation fuels.  
56        The measurements were conducted during two separate test campaigns performed three years apart,  
57        each employing a different regulatory compliant sampling and measurement reference system for  
58        aircraft engine nvPM emissions. The objective was to investigate the correlation of fuel hydrogen  
59        content with nvPM number and mass emissions at the engine exit plane (EEP) independent of fuel  
60        composition, measurement system, and ambient conditions. The nvPM number and mass emissions  
61        and size distributions systematically decreased with increasing fuel hydrogen content regardless of  
62        the fuel composition or APU operating condition. The measured nvPM emissions were particle loss-  
63        corrected to the EEP and normalised to a common fuel hydrogen content. Similar rates of nvPM  
64        reductions were observed for both test campaigns at all investigated APU operating conditions,  
65        confirming that engine exit nvPM reductions correlate with fuel hydrogen content for fuels of  
66        relatively similar compositions. This analysis method can be applied to emissions data from other  
67        engine types to compare the reduction in nvPM emissions for sustainable aviation fuels and blends.

68

69

70

71        **Keywords:** Aircraft emissions, non-volatile Particulate Matter, Sustainable Aviation Fuel, Auxiliary  
72        Power Unit, Fuel hydrogen content, Particle loss correction.

## 73 **1. Introduction**

74 Aviation is an essential mode of transportation in the modern world, connecting nations, economies,  
75 and facilitating the transportation of goods. The air transportation industry has been estimated to  
76 provide about twelve million skilled jobs and contributes over 700 billion euros to Europe's economy  
77 [1], with a global average annual growth rate of 2% forecasted between 2017 and 2040 for aircraft  
78 movements [2]. The aviation sector is a fast-growing source of greenhouse gas emissions, currently  
79 representing 1.7-2.3% of global carbon emissions [3]. In a globalised world facing the consequences  
80 of climate change, deterioration of local air quality, and increased scarcity of resources, the  
81 continuous growth of aviation has led to extensive research and development towards more fuel-  
82 efficient engine technologies, and sustainable aviation fuel (SAF) sources to reduce the environmental  
83 impact. To address CO<sub>2</sub> emissions from international aviation and consistent with the aviation  
84 industry's commitment to carbon neutral growth from 2020, the International Civil Aviation  
85 Organization (ICAO) implemented the Carbon Offsetting and Reduction Scheme for International  
86 Aviation (CORSIA), a global market-based measure [4].

87 Aircraft gas turbine engines emit ultrafine Particulate Matter (PM) typically <100 nm in mean diameter  
88 [5–8]. Within the boundary layer, these emissions are associated with reduced air quality and have  
89 the potential for adverse health impacts in the vicinity of airports [9–11]. Aircraft gas turbine engines  
90 are also the main anthropogenic source of PM emissions in the upper atmosphere at cruising altitudes  
91 [12], with soot contributing to contrail cirrus formation and radiative forcing [12–14].

92 In order to mitigate the impact of aircraft engine PM emissions, ICAO has recently adopted new  
93 regulatory methodology for the sampling and measurement of aircraft engine nvPM mass and number  
94 emissions, with a new nvPM mass regulatory standard effective 1 January 2020 for in-production  
95 turbofan and turbojet engines with rated thrust greater than 26.7 kN [15]. Aircraft engine nvPM is  
96 defined as particles exiting an aircraft engine that do not volatilise when heated to a temperature of  
97 350°C and consist essentially of soot or black carbon [15]. When measuring aircraft engine nvPM

98 emissions, the extracted exhaust aerosol must be diluted and cooled, in order to suppress condensation  
99 and nucleation of volatile species present in the gas phase, before being transported and analysed by  
100 diagnostic instruments [16]. A standardised sampling and measurement system has been developed  
101 by the Society of Automotive Engineers (SAE) Aircraft Engine Gas and Particulate Emissions  
102 Measurement (E-31) committee [16] and adopted by ICAO as described in “*Annex 16 – Environmental*  
103 *Protection Volume 2 – Aircraft Engine Emissions*” to the Convention on International Civil Aviation [15].  
104 The development of this standardised methodology, described in SAE Aerospace Recommended  
105 Practice (ARP) 6320 [16], was achieved using results of multiple aircraft engine emission tests and  
106 experimental work conducted primarily during the Studying, sAmpling and Measuring of aircraft  
107 ParticuLate Emissions (SAMPLE) campaigns [17–23] and Aviation-Particle Regulatory Instrumentation  
108 Demonstration Experiment (A-PRIDE) [24,25] programmes.

109 While the new regulatory standard specifies systematic measurement of aircraft engine nvPM  
110 emissions at the instrument location, the sampling system requirements coupled with the small  
111 particle mean diameters observed from aircraft engines [5–8] result in a significant size-dependent  
112 particle losses of up to 90% for nvPM number and 50% for nvPM mass [15,26], prior to the  
113 measurement by the calibrated instruments. The nvPM mass and number concentrations at the  
114 Engine Exit Plane (EEP) can be estimated by accounting for these physical losses in the sampling and  
115 measurement system.

116 Aircraft engine nvPM emissions are influenced by the underlying physical properties and chemical  
117 composition of the fuel being burned, especially the fuel aromatic content, which varies globally by  
118 several percent for conventional jet fuel [27,28]. Sustainable aviation fuels are increasingly being  
119 sought as replacements for conventional fossil fuels, which have additional benefits in terms of lower  
120 emissions [29–32], reduced contrail formation [33], and improved local air quality in the vicinity of  
121 airports [34]. The blending of conventional jet fuels with synthetic paraffinic fuels have been shown  
122 to reduce aircraft engine nvPM emissions, that scale inversely with higher fuel hydrogen content and

123 lower fuel aromatic content [35]. It has also been shown that for a fuel blend which would meet  
124 current ASTM International specifications, a reduction in nvPM number-based emissions of ~35% and  
125 nvPM mass-based emissions of ~60% could be achieved for an aircraft auxiliary power unit (APU) [36].

126 In 2012, the European Commission funded a collaborative research project - Initiative Towards  
127 sustAinable Kerosene for Aviation (ITAKA). The main objectives of the ITAKA project were to (1)  
128 develop a full value-chain in Europe to produce sustainable drop-in hydrotreated esters and fatty acids  
129 (HEFA) fuels and study the implications of a large-scale use, and (2) conduct research on sustainability,  
130 economic competitiveness, and technology readiness [37]. The ITAKA project primarily targeted  
131 camelina oil as the most promising sustainable feedstock, with used cooking oil (UCO) as an alternative  
132 feedstock. Both feedstocks were converted to drop-in aviation fuels through the HEFA pathway.

133 As part of the ITAKA project framework, the impact of fuel composition on the nvPM emissions of a  
134 Garrett Honeywell GTCP85 APU were investigated at three operating conditions burning blends of Jet  
135 A-1 and alternative fuels produced from UCO and Camelina feedstocks. The emissions measurements  
136 were performed at the University of Sheffield Low Carbon Combustion Centre during two distinct test  
137 campaigns conducted in June 2014 (ITAKA 1) and April 2017 (ITAKA 2). Measurements were  
138 independently performed utilising the standardized North American and European reference  
139 sampling and measurement systems, respectively, with additional measurements of particle size  
140 distributions obtained to facilitate particle loss correction estimates. During ITAKA 1, 16 blends of  
141 UCO-HEFA with conventional Jet A-1 were investigated, while 12 blends of Camelina-HEFA and  
142 conventional Jet A-1 were used during ITAKA 2. Details of the ITAKA 1 test campaign have been  
143 previously reported [36,38]. Particle size distribution measurements were used to correct the  
144 measured nvPM emissions data for particle losses in the sampling and measurement system, to  
145 provide an estimate of the nvPM emissions at the EEP. The impact of fuel composition on nvPM  
146 number and mass emissions reductions was subsequently assessed using the EEP data.

## 147 **2. Experimental Methods**

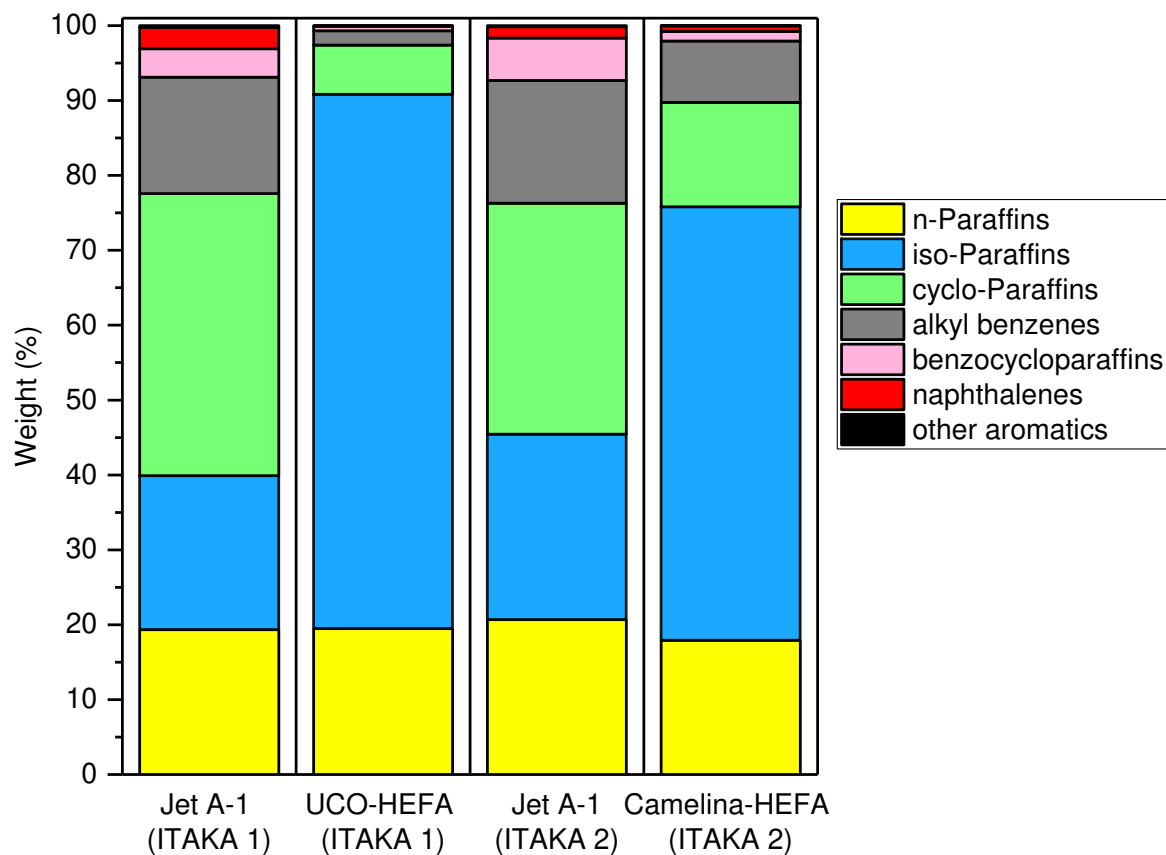
148 **2.1. Fuels**

149 The 18 fuels investigated during the ITAKA 1 campaign were derived from a conventional Jet A-1 and  
 150 neat UCO-HEFA, with 16 blends of the two fuels mixed in different proportions. During the ITAKA 2  
 151 campaign, 14 fuels derived from a different Jet A-1 and pure Camelina-HEFA fuel were studied with  
 152 12 blends of the two fuels mixed at ratios of 10, 20, 30, 35, 40, 50, 60, 70, 80, 85, 90, 95%, by mass.  
 153 The properties of specific Jet A-1 and alternative fuels (UCO-HEFA and Camelina-HEFA) used during  
 154 the two ITAKA test campaigns are presented in **Table 1**. It should be noted that the UCO-HEFA and  
 155 Camelina-HEFA fuels had a higher net heat of combustion and a higher hydrogen content compared  
 156 to Jet A-1. The fuel hydrogen content was evaluated using two different methods: ASTM D5291 and  
 157 two-dimensional gas chromatography (GCxGC) analysis. For the same fuel, differences of 0.05-0.1% in  
 158 hydrogen content were reported. In this study, for consistency, only fuel hydrogen content derived  
 159 from GCxGC data is reported which was used in turn to determine the H/C ratio required to calculate  
 160 nvPM number and mass emission indices, and for subsequent data analysis. The GCxGC analysis was  
 161 performed using stored volumes of fuels by the same accredited laboratory (Intertek) for all four fuels.

162 **Table 1: Selected properties of the neat fuels used in the ITAKA test campaigns**

Test campaign	ITAKA 1			ITAKA 2		
	Method	Jet A-1	UCO-HEFA	Method	Jet A-1	Camelina-HEFA
Density at 15°C [kg/m <sup>3</sup> ]	IP365	805.3	759.6	IP365/D4052	806.7	779.6
Distillation temperature [°C]						
10% boiling point	ASTM D86	163.8	169.8	ASTM D86	171.0	173.2
90% boiling point	ASTM D86	236.4	235.1	ASTM D86	238.3	262.8
Final boiling point	ASTM D86	259.1	251.9	ASTM D86	259.8	274.6
Net heat of combustion [MJ/kg]	ASTM D3338	43.153	44.023	ASTM D3338	43.23	43.695
Smoke point [mm]	ASTM D1322	23	>50	ASTM D1322	23	35.5
Kinematic viscosity at -20°C [mm <sup>2</sup> /s]	IP71	3.521	3.885	D445	3.887	5.107
Sulphur [mass %]	ASTM D4294	0.033	<0.018	D4294/D2622	0.150	0.070
Hydrogen [weight %]	Calculated from GCxGC	13.94	15.22	Calculated from GCxGC	14.00	14.80
H/C ratio	Calculated from GCxGC	1.93	2.14	Calculated from GCxGC	1.94	2.07

164 The GCxGC analysis of fuel composition of the Jet A-1, UCO-HEFA, and Camelina-HEFA fuels is  
 165 presented in **Figure 1**. The two Jet A-1 fuels used in the ITAKA 1 and 2 campaigns were different, but  
 166 each had a distribution of hydrocarbon groups typically found in conventional fuels. The UCO-HEFA  
 167 and Camelina-HEFA fuels have a higher proportion of iso-Paraffins and lower proportion of cyclo-  
 168 Paraffins, alkyl benzenes and benzo-cycloparaffins compared to the Jet A-1 fuels.



169

170 **Figure 1: Chemical composition of conventional and alternative fuels obtained from GCxGC**  
 171 **analysis**

172 **2.2. Ambient conditions**

173 Aircraft engine PM emissions can be affected by ambient conditions. An increase in ambient  
 174 temperature has been shown to reduce aircraft engine total PM emissions as the warmer ambient air  
 175 is thought to mitigate volatile aerosol formation [29,39]. However, the influence of ambient  
 176 environmental conditions on nvPM formation within a gas turbine engine has received little attention

177 and is currently poorly understood [24]. Ambient temperature, ambient pressure, and relative  
 178 humidity were recorded during the two test campaigns with measured ranges presented in **Table 2**.  
 179 The ambient conditions were significantly different between the ITAKA 1 and ITAKA 2 campaigns, with  
 180 a median difference of 10.6°C, 38.8 mbar, and 19.5%, in temperature, pressure, and relative humidity,  
 181 respectively.

182 **Table 2: Ambient conditions recorded during the ITAKA 1 and ITAKA 2 test campaigns**

	Temperature (°C)	Pressure (mbar)	Relative Humidity (%)
ITAKA 1	14.0 – 20.6	1024.7 – 1031.1	61 – 85
ITAKA 2	4.5 – 6.1	987.2 – 990.9	86 – 99

183

### 184 **2.3. APU Operating conditions**

185 During the ITAKA 1 and ITAKA 2 test campaigns, the same Garrett Honeywell GTC85 APU was used as  
 186 the source of emissions. It was operated at three conditions: No Load (NL), Environmental Control  
 187 Systems (ECS), and Main Engine Start (MES). These three conditions correspond to the normal  
 188 operating conditions for an APU. At each stable APU operating condition, parameters such as fuel flow  
 189 rate, air-to-fuel ratio (AFR), and exhaust gas temperature (EGT) were recorded. The typical APU  
 190 operational parameters recorded during Jet A-1 runs in both test campaigns are presented in **Table 3**.  
 191 The APU operational parameters were highly reproducible and stable during both test campaigns,  
 192 with the average fuel flow rate, AFR, and EGT all within one standard deviation of the mean.

193 **Table 3: APU operational parameters at different operating conditions for Jet A-1 runs**

Test campaign	ITAKA 1	ITAKA 2	ITAKA 1	ITAKA 2	ITAKA 1	ITAKA 2
Operating condition	NL		ECS		MES	
Fuel flow rate (g/s)	17.7 ± 0.2	17.8 ± 0.2	25.8 ± 0.3	25.9 ± 0.2	31.1 ± 1.1	31.8 ± 0.4
AFR	135.0 ± 3.9	135.9 ± 3.9	84.4 ± 0.8	84.4 ± 0.8	62.2 ± 1.0	62.2 ± 1.0
EGT (°C)	324.1 ± 6.0	323 ± 3.7	475.2 ± 5.0	475.8 ± 4.6	600.0 ± 7.6	604.3 ± 6.2

194

### 195 **2.4. nvPM Sampling and measurement systems**

196 For all tests reported here, the exhaust aerosol produced by the APU was extracted via a single-point  
 197 stainless probe, 3/8'' in outer diameter (0.0035'' wall) positioned within ½ nozzle diameter of the APU

198 exit plane (~100 mm). Downstream of the probe, the North American and European reference  
199 sampling and measurement systems were used during the ITAKA 1 and ITAKA 2 campaigns,  
200 respectively, to quantify nvPM mass-based emissions, nvPM number-based emissions, and particle  
201 size distributions. Both reference systems were operated in compliance with ICAO standard  
202 methodology specified in Appendix 7 of Annex 16 [15] and in SAE ARP 6320 [16]. These reference  
203 systems had similar measurement characteristics with minimal differences in employed number and  
204 mass analysers, system dimensions, flowrates, and temperatures. The North American mobile  
205 reference system was operated by the Missouri University of Science and Technology and has been  
206 described previously [24,25,30]. The European mobile reference system was operated by Cardiff  
207 University with further details described elsewhere [21,22,25]. A general description of the  
208 experimental set-up employed during both test campaigns is presented here: APU emissions entered  
209 the sampling systems via the aforementioned 3/8" stainless steel probe and 7.5 m long (7.75 mm inner  
210 diameter (ID) stainless-steel heated line maintained at 160°C. The sampled aerosol was then split into  
211 three lines namely a diluted nvPM line, an undiluted line for the measurement of smoke number and  
212 gaseous emissions (CO<sub>2</sub>, CO, and NO<sub>x</sub>), and a pressure relief line. The nvPM sample was then diluted  
213 using an ejector diluter (Dekati DI-1000) using dry nitrogen cooling the nvPM sample to 60°C whilst  
214 suppressing the potential for particle coagulation, water condensation, and volatile particle formation  
215 in the sample lines. The dilution factor was derived from raw (gas line) and diluted (nvPM line) CO<sub>2</sub>  
216 concentrations, which were measured using a suitably ranged NDIR CO<sub>2</sub> analyser as specified by ARP  
217 6320 [16]. A 25 m long anti-static polytetrafluoroethylene (PTFE) sample line maintained at 60°C  
218 transported the diluted aerosol to the nvPM analysers. A 1 µm sharp-cut cyclone was placed prior to  
219 the measurement analysers for protection and to limit line shedding interference. The nvPM number  
220 concentration was measured using an AVL Particle Counter (APC) Advanced consisting of a n-butanol  
221 based TSI 3790E Condensation Particle Counter (CPC) and a volatile particle remover (VPR) consisting  
222 of a catalytic stripper in between a two-stage rotary diluter and a porous tube diluter to remove  
223 volatile particles and further dilute the sample. The nvPM mass concentration was measured using an

224 AVL Micro Soot Sensor (MSS) and an Artium Laser Induced Incandescence LII 300, however, to enable  
225 comparison, only data from the MSS is reported here.

226 During both test campaigns, in compliance with ICAO Annex 16 [15], the dilution factor was  
227 maintained in the range 8-14, averaging  $11.7 \pm 1.3$  during ITAKA 1 and  $10.7 \pm 0.8$  during ITAKA 2.  
228 Performance evaluation and comparison of the North American and European standardized reference  
229 systems for the measurement of aircraft engine nvPM number and mass emissions has been  
230 previously established using a CFM56-7B26/3 engine [22,25].

231 Additional particle size distribution (PSD) measurements, currently not prescribed by the ICAO  
232 standard methodology, were performed using calibrated DMS 500 fast-mobility spectrometers  
233 (Cambustion Ltd). The DMS 500 provides a measure of the particle size distribution in terms of  
234 electrical mobility, and has been frequently used to report size distribution characteristics of aircraft  
235 engine PM emissions [36,40,41]. In this analysis, it was ensured that consistent inversion matrices  
236 were selected to allow comparative size distribution data between the two test campaigns.

## 237 **2.5. Test matrix and measurement methodology**

238 The APU was initially put through a warmup sequence prior to operation with different fuels. For each  
239 fuel tested, one test cycle corresponded to a stair-wise step down from MES to ECS to NL, which was  
240 repeated once without APU shutdown. This procedure minimised differences in the APU temperature  
241 and, hence, potential differences in the fuel vaporization rate that may contribute to measurement  
242 uncertainties. Blends of Jet A-1 and alternative fuels were randomly selected (non-sequential) to  
243 mitigate potential bias and drift. The nvPM emissions using neat Jet A-1 were recorded daily and used  
244 as a baseline to monitor the APU performance and measurement system repeatability during each  
245 campaign. Cleanliness and background checks for the nvPM number and mass analysers were also  
246 performed daily in conformity with standard methodology [15].

247 Each nvPM data point corresponds to an average of at least two (up to six for Jet A-1) repeats recorded  
248 over stable periods of 30 seconds to 2 minutes. At stable APU operating conditions, the averaged

249 Coefficient of Variation (CV) over both test campaigns was  $1.1 \pm 0.4\%$  for nvPM number concentration  
 250 and  $3.3 \pm 1.5\%$  for nvPM mass concentration.

## 251 **2.6. nvPM Data analysis (Emission Indices and particle loss correction)**

252 The nvPM number and mass emissions are reported as Emission Indices (EIs) at the measurement  
 253 location and at the EEP. The EI metric is used to assess the engine emissions for different operating  
 254 conditions per unit mass of fuel burned [15,16], with the simplified equations for the EIs at the  
 255 measurement location given below:

$$\mathbf{EI}_{\text{number-meas}}[\#/kg_{\text{fuel}}] = \frac{\text{nvPM}_{\text{num-STP}} \times \text{DF}_2 \times 22.4 \times 10^6}{CO_{2\text{dil}} \times (M_C + \alpha \times M_H)} \quad (1)$$

$$\mathbf{EI}_{\text{mass-meas}}[g/kg_{\text{fuel}}] = \frac{\text{nvPM}_{\text{mass-STP}} \times 22.4 \times 10^{-6}}{CO_{2\text{dil}} \times (M_C + \alpha \times M_H)} \quad (2)$$

256 With “ $\text{nvPM}_{\text{num-STP}} \times \text{DF}_2$ ” the secondary stage dilution (in the VPR) corrected number concentration in  
 257 particles/cm<sup>3</sup> corrected to Standard Temperature and Pressure (STP: 0°C and 101.325 kPa),  $\text{nvPM}_{\text{mass-STP}}$   
 258 the measured mass concentration in  $\mu\text{g}/\text{m}^3$  corrected to STP,  $CO_{2\text{dil}}$  the diluted  $CO_2$  concentration  
 259 at the number and mass analysers in molar fraction,  $M_C$  and  $M_H$  the molar masses of carbon and  
 260 hydrogen, respectively, and  $\alpha$  the hydrogen to carbon (H/C) ratio of the fuel.

261 The EEP nvPM number and mass EIs were calculated from measured EIs by correcting for particle loss  
 262 using equation (3).

$$\mathbf{EI}_{\text{EEP}} = \mathbf{EI}_{\text{meas}} \times k_{\text{SL}} \times k_{\text{thermo}} \quad (3)$$

263 where  $\mathbf{EI}_{\text{meas}}$  is the measured nvPM number/mass EI calculated using equation (1) and (2),  $k_{\text{thermo}}$  is the  
 264 thermophoretic particle loss correction factor for the extraction section of the sampling system  
 265 [15,16], and  $k_{\text{SL}}$  is the system particle loss correction factor (excluding thermophoretic loss in the  
 266 extraction section) as discussed below. It should be noted that given the scope of this paper was to  
 267 compare the nvPM emissions reported by the two reference systems, the energy content of the fuel  
 268 was not considered. However, fuel energy content correction should be included when assessing the

269 impact of fuel composition on local air quality, since for the same operating condition different mass  
270 flow rate of fuel would need to be burned. For the fuels investigated in this study, the HEFA fuels had  
271 a higher energy content which would have corresponded to a small reduction in emitted nvPM ( $\leq 2\%$ ).  
272 Historically, loss correction factors have been experimentally determined by measuring particle size  
273 distributions upstream and downstream of a sampling system [8,39,42,43]. When particle size  
274 distribution measurements at both ends of the sampling system are not possible, a particle loss  
275 correction factor can be estimated using the United Technologies Research Center (UTRC) particle  
276 transport model predicting size-dependent particle loss based on sampling system configuration data,  
277 as described in SAE AIR 6504 [44]. The UTRC model can be combined together with the measured  
278 particle effective density and the measured particle size distribution to estimate EEP number and mass  
279 emissions [7,40,45]. In this analysis, the system loss correction factors ( $k_{SL}$ ) for nvPM number and mass  
280 were determined using the measured particle size distributions and the UTRC model as follows: For  
281 each sampling system, the number, mass, and size loss functions ( $f_{loss}$ ) were determined by combining  
282 the particle losses in the system determined using the UTRC model with VPR, CPC, and cyclone  
283 penetration functions derived from calibration data and manufacturer specifications, as discussed in  
284 Appendix 8 of ICAO Annex 16 [15]. In this context, the loss functions  $f_{loss}$  represents size-dependent  
285 losses of the sampled particles between the sampling system inlet (i.e. EEP) and the analysers (i.e.  
286 measurement location). Particle size distributions were estimated at the EEP by dividing the measured  
287 size distributions by the predicted loss function ( $PSD_{EEP} = PSD_{measured}/f_{loss}$ ). System loss  
288 correction factors ( $k_{SL}$ ) were obtained by dividing the nvPM number/mass concentration derived from  
289 the particle size distribution at the nvPM number/mass analyser location with the nvPM number/mass  
290 concentration derived from the particle size distribution at the EEP. For the calculation of the nvPM  
291 mass correction factors, nvPM number-based size distributions were converted into mass-based size  
292 distributions using equation (4), and assuming particle sphericity and an effective density of  $1 \text{ g/cm}^3$   
293 as typically assumed for aircraft engine nvPM [26,40].

$$\text{Mass}(d_p) = \text{Number}(d_p) \times \text{Volume}(d_p) \times \rho_{\text{eff}}(d_p) = \frac{\text{Number}(d_p) \times \pi \times \rho_{\text{eff}}(d_p) \times d_p^3}{6} \quad (4)$$

294

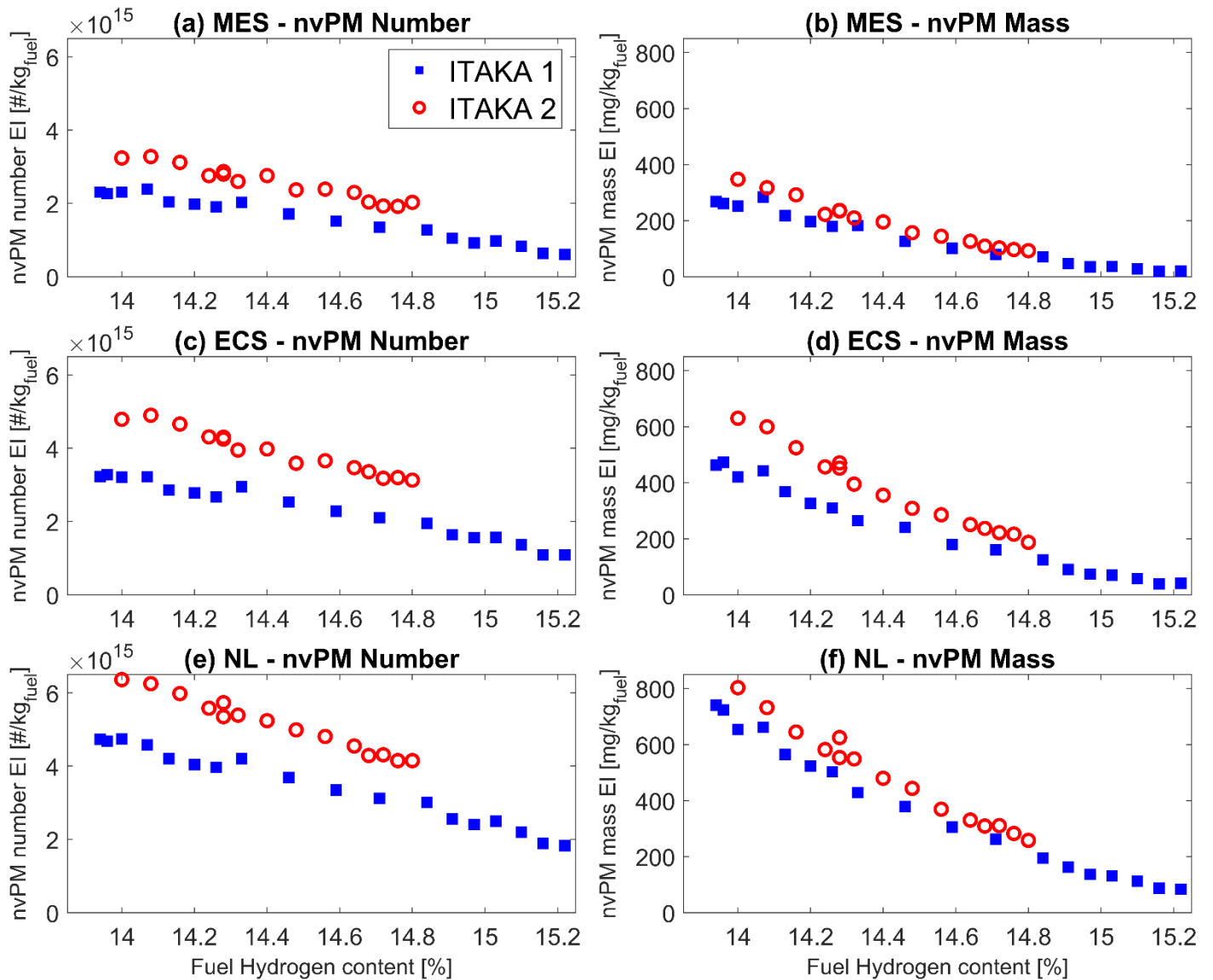
295 Other characteristic parameters were derived from the EEP-estimated particle size distributions, such  
296 as the number-based geometric mean diameter (GMD) and geometric standard deviation (GSD) to  
297 compare the data from the two campaigns in terms of particle size-related parameters.

### 298 **3. Results and discussion**

#### 299 **3.1. Measured nvPM emissions**

##### 300 **3.1.1. Measured nvPM number and mass**

301 The nvPM number and mass EIs measured during the two ITAKA test campaigns across the range of  
302 fuel blends and APU operating conditions are presented in **Figure 2**. The fuel hydrogen content was  
303 selected as the parameter to compare the data from the two campaigns, as it has been shown to  
304 better correlate with sooting propensity than the fuel aromatic content [32,35,45].



306 **Figure 2: Measured nvPM number- (a)(c)(e) and nvPM mass- (b)(d)(f) -based EIs as a function of**  
 307 **fuel hydrogen content for the three APU operating conditions**

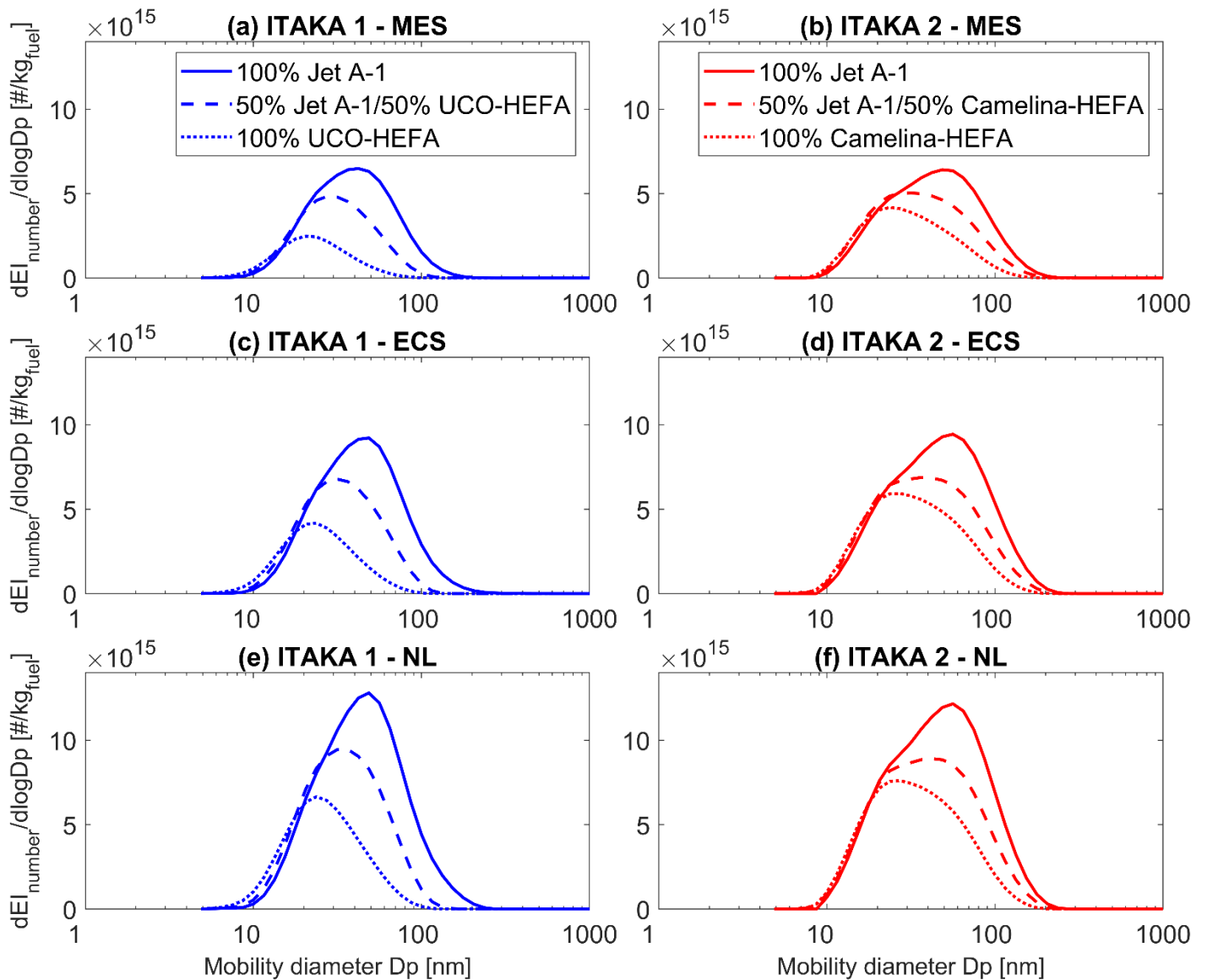
308 The nvPM number and mass EIs at the measurement location for both test campaigns are observed  
 309 to decrease with increasing fuel hydrogen content regardless of the fuel composition or APU operating  
 310 condition, in agreement with the literature [32,36,45]. When comparing campaign specific nvPM  
 311 emissions at the different APU operating conditions (**Figure 2 (a)-(c)-(e) and (b)-(d)-(f)**), the nvPM  
 312 number and mass EIs decrease with increasing APU fuel flow rate (corresponding to the different  
 313 operating conditions (**Table 3**)), suggesting that the APU combustion efficiency increases from NL to  
 314 ECS to MES as has been previously observed [36].

315 For a given fuel hydrogen content, the nvPM EIs at the measurement location reported for the ITAKA  
316 2 campaign are consistently higher, on average 28% for nvPM number and 15% for nvPM mass across  
317 the three APU power conditions. As discussed in previous work [25], the expected levels of uncertainty  
318 in certified nvPM EI mass and number measurement are 22% and 25% respectively, with empirically  
319 derived data during parallel measurement of three ICAO compliant sampling systems on a CFM56-  
320 7B26/3 engine found to be within these bounds. In addition to the certified nvPM measurement  
321 uncertainty, the observed differences between ITAKA 1 and ITAKA 2 can be further explained by: - the  
322 different ambient conditions (**Table 2**) with the lower ambient temperature recorded during ITAKA 2  
323 inducing lower quenching temperature and hence higher soot production, - engine wear between the  
324 two test campaigns - different fuel compositions (**Table 1** and **Figure 1**), - spatial inhomogeneity of the  
325 exhaust stream (i.e. different sampling location of the probe in the exhaust stream).

326 It should be noted that the repeatability associated with nvPM measurement specific to each test  
327 campaign was quantified by repeating daily measurements using the conventional Jet A-1 (up to 6  
328 repeats per test campaigns), with a standard deviation of  $\leq 5.1\%$  for measured nvPM number EI and  
329  $\leq 4.7\%$  for measured nvPM mass EI.

### 330 **3.1.2. Measured particle size distributions**

331 The typical EI-weighted particle size distributions measured with a DMS 500 during ITAKA 1 and ITAKA  
332 2 for selected fuels at the three APU operating conditions are presented in **Figure 3**, from which the  
333 statistical GMD and GSD were calculated at the measurement location, the GMD varied from 22.6 to  
334 43.0 nm with a GSD of 1.59 – 1.78 for the ITAKA 1 dataset, and for ITAKA 2, the GMD ranged from 30.1  
335 to 44.9 nm with a GSD of 1.77 – 1.9. The nvPM number concentration (obtained from integrating the  
336 area under the particle size distribution) and GMD are observed to decrease with increasing  
337 proportion of alternative fuel (i.e. higher fuel hydrogen content) and increasing fuel flow rate (**Table**  
338 **3**).



340 **Figure 3: “EI number”-weighted particle size distributions at the measurement location for**  
 341 **different fuel blends and for the three APU operating conditions**

342 The particle size distributions at the measurement location generally appear monomodal and near  
 343 lognormal, with a good correlation between the two test campaigns. However, for some conditions a  
 344 small shoulder can be observed at  $\approx 20$  nm thought to be an artifact of the DMS-500 inversion matrix  
 345 for the calibration file used.

346 **3.2. Engine exit plane nvPM emissions**

347 Currently, the nvPM number and mass EIs at the measurement location (corrected for size-  
348 independent thermophoretic loss in the aerosol extraction section of the sampling system) are used  
349 for aircraft engine emissions certification [15]. Size-dependent particle losses are not factored into the  
350 EIs reported for emissions certification. This would therefore lead to an underestimation of EEP EIs  
351 and bias the impact of fuel composition on nvPM emissions produced by the engine. Particle-loss-  
352 corrected EEP concentrations as would be required for airport emissions inventories, and  
353 environmental impact assessment, are therefore essential to better interpret the overall impact of  
354 fuel composition on nvPM number and mass emissions reduction.

### 355 **3.2.1. Particle loss correction factors**

356 The nvPM number and mass loss correction factors used to predict the EEP nvPM emissions, and  
357 calculated as described in section 2.6 are presented in **Table 4**. As expected,  $k_{SL_{number}}$  is observed to  
358 be larger than  $k_{SL_{mass}}$  given the higher diffusion losses reported at smaller sizes. A broader range of  
359 correction factors were calculated for the ITAKA 1 dataset as a consequence of the smaller GMDs and  
360 GSDs as well as broader range of fuel blends investigated relative to the ITAKA 2 campaign (**Figure 3**).  
361 It should be noted that the system loss corrections factors were generally higher at the highest APU  
362 operating condition (MES) because of the generally smaller mean particle diameter observed at this  
363 condition.

364 **Table 4: System loss correction factors for the two test campaigns**

Test campaign	$k_{SL_{number}}$	$k_{SL_{mass}}$
ITAKA 1	2.21 – 4.70	1.13 – 1.40
ITAKA 2	2.32 – 3.40	1.12 – 1.20

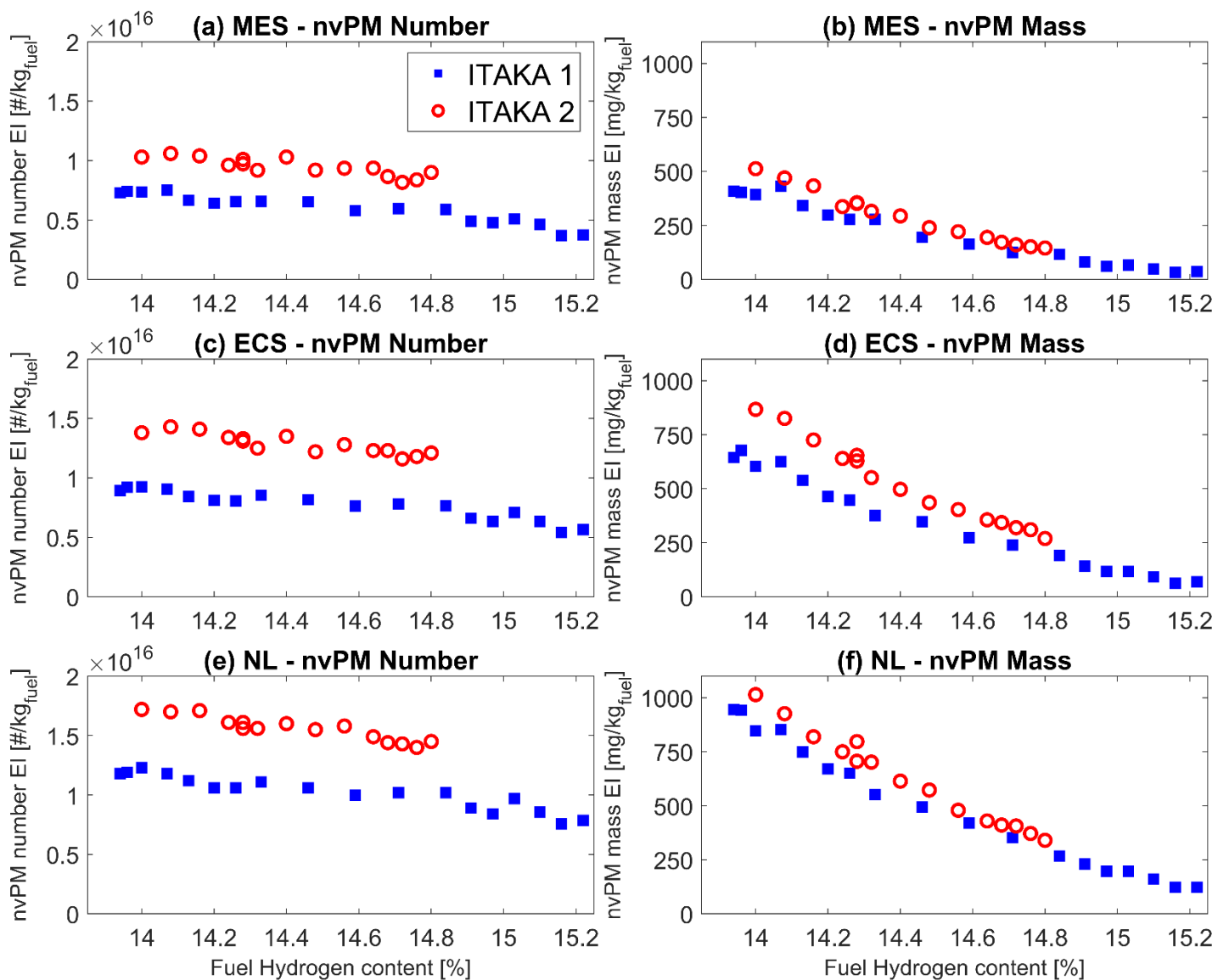
365

### 366 **3.2.2. nvPM number and mass emissions**

367 The particle-loss-corrected EEP nvPM number and mass EIs for the two campaigns are presented in  
368 **Figure 4**. As expected and in agreement with the measured nvPM EIs (**Figure 2**), EEP nvPM number  
369 and mass EIs are observed to reduce with increasing fuel hydrogen content. However, EEP nvPM EIs

370 are higher than the corresponding nvPM EIs at the measurement location, on average 70% for number  
 371 ( $\leq 84\%$ ) and 30% for mass ( $\leq 45\%$ ), in agreement with the standard methodology [44].

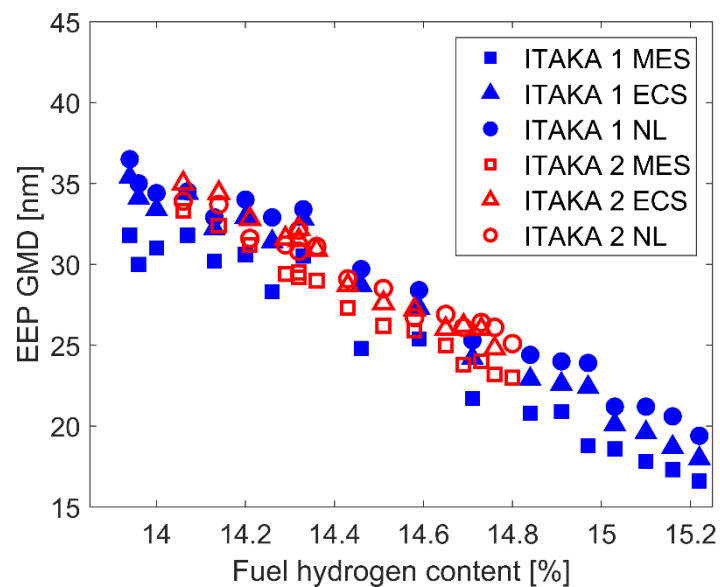
372 Similar to what was observed with measured nvPM emissions (section 3.1.1), the calculated EEP nvPM  
 373 EIs remain consistently larger during ITAKA 2 for a given fuel hydrogen content when compared to  
 374 ITAKA 1, with particle loss correction not having a significant effect on this trend.



376 **Figure 4: Engine exit plane (EEP) corrected nvPM number- (a)(c)(e) and nvPM mass- (b)(d)(f) -based**  
 377 **EIs as a function of fuel hydrogen content for the three APU operating conditions**

378 **3.2.3. GMD and GSD**

379 The particle size distribution parameters, GMD and GSD, were computed from the EEP-corrected  
 380 particle size distributions and evaluated as a function of fuel hydrogen content. A decrease in GMD  
 381 was observed with increasing fuel hydrogen content at the three APU operating conditions for both  
 382 test campaigns (**Figure 5**), with EEP GMDs varying 16.6 – 36.5 nm for ITAKA 1 and 23.0 – 35.4 nm for  
 383 ITAKA 2. The reduction in EEP GMD with increasing fuel hydrogen content is consistent between the  
 384 two test campaigns (**Figure 5**), highlighting that fuel hydrogen content is also a strong correlating  
 385 parameter for mean particle size reduction. The correlation between GSD and fuel hydrogen content  
 386 was less apparent with a small reduction observed for ITAKA 2 (GSD: 1.79 – 2.02) and no correlation  
 387 observed for ITAKA 1 (GSD: 1.68 – 1.88).



388  
 389 **Figure 5: Geometric Mean Diameter from the EEP-corrected particle size distributions as a function**  
 390 **of fuel hydrogen content**

391  
 392 **3.3. Normalised engine exit plane nvPM emissions**

393 As seen in **Figure 1** and **Table 1**, the jet A-1 fuels and alternative fuels in ITAKA 1 and ITAKA 2 campaigns  
 394 had different chemical compositions. As such, in order to isolate the specific impact of fuel  
 395 composition on nvPM emissions reduction observed during the two campaigns, whilst minimising

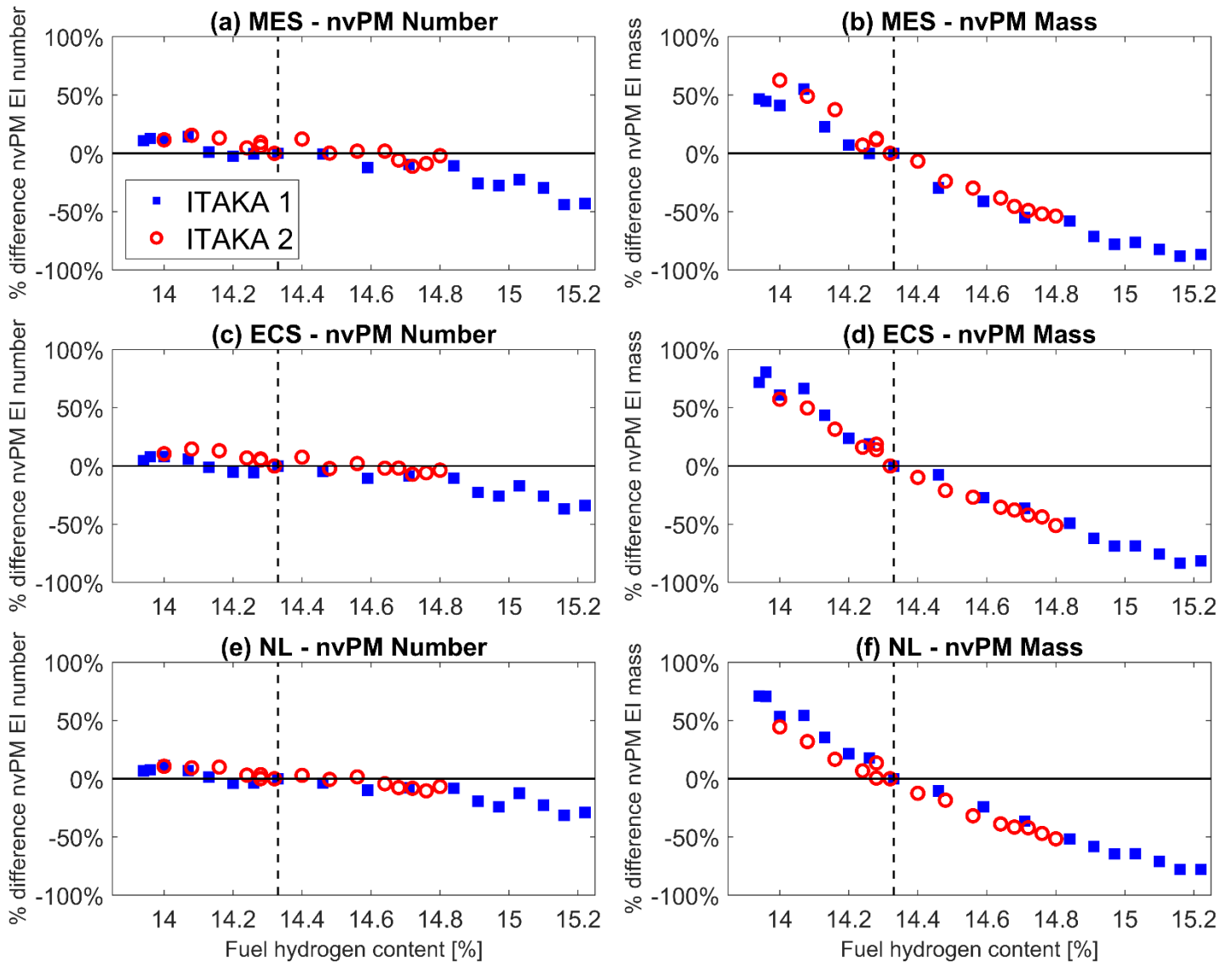
396 uncertainties associated with engine wear, measurement uncertainty, ambient conditions, and  
397 sampling representativeness, the EEP nvPM data was normalised to a common fuel hydrogen content  
398 measured for both ITAKA test campaigns (i.e. 14.33%). The data was presented as a percent difference  
399 in EEP nvPM EI relative to Jet fuel with  $H_{\text{content}} = 14.33\%$ , as defined in equation (5).

$$\text{Percent difference (relative to } H_{\text{content}} = 14.33\%) = 1 - \frac{\text{EEP nvPM EI}_{H_{\text{content}} = X\%}}{\text{EEP nvPM EI}_{(H_{\text{content}} = 14.33\%)}} \quad (5)$$

400 It should be noted that the data was normalised to a nominally similar fuel hydrogen content reported  
401 for both campaigns and not to the conventional Jet A-1 as was previously performed for ITAKA 1 [36].  
402 This approach accounts for the fact that the expected nvPM emissions vs. fuel hydrogen content  
403 correlations are non-linear, and that the Jet A-1 fuels used in ITAKA 1 and 2 had different fuel hydrogen  
404 contents (**Table 1**).

### 405 **3.3.1. nvPM number and mass reductions**

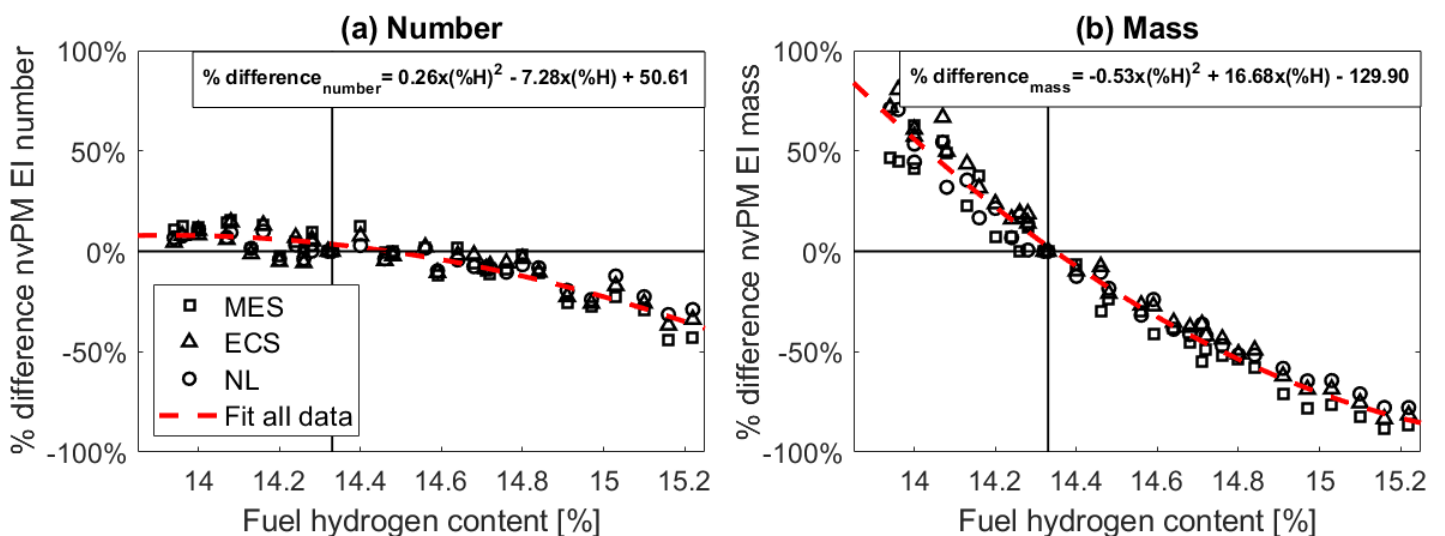
406 Percentage reductions of EEP-corrected nvPM EIs (normalised to the 14.33% fuel hydrogen content  
407 datum) as a function of fuel hydrogen content are presented in **Figure 6** for the two campaigns. Similar  
408 to the EIs at the measurement location and EEP, the normalised EEP nvPM EIs were observed to  
409 decrease with increasing fuel hydrogen content for both ITAKA campaigns. The EEP nvPM mass EI  
410 percentage reduction with increasing fuel hydrogen content were significantly higher than that of the  
411 EEP nvPM number EI, which can be explained by the fact that the particle size distribution shifted to  
412 smaller sizes (**Figure 5**), which affects nvPM mass emissions more than nvPM number emissions. These  
413 results indicate that the fuel hydrogen content is a suitable correlating parameter for nvPM reduction  
414 adequately capturing differences in fuel composition for the two HEFA fuels and blends used in the  
415 ITAKA 1 and 2 campaigns.



417 **Figure 6: Percent difference in EEP-corrected nvPM number- (a)(c)(e) and nvPM mass- (b)(d)(f) -**  
 418 **based emission indices (relative to 14.33% fuel hydrogen content data) as a function of fuel**  
 419 **hydrogen content for the three APU operating conditions**

420 Since the trend and magnitude of EEP nvPM percentage reductions for each of the three APU  
 421 operating conditions during both campaigns were similar, the overall percent difference in nvPM  
 422 emissions for the GTCP85 APU was further assessed by combining the data from the two campaigns  
 423 **(Figure 7)**. The EEP nvPM EI percentage differences for both test campaigns at all three APU operating  
 424 conditions are observed to be in good statistical agreement, as evidenced by the high coefficient of  
 425 determination values for the second order polynomial fit to the data ( $R^2=0.84$  for nvPM number and

426  $R^2=0.97$  nvPM mass), and by the relatively low average difference between the fit and the measured  
 427 data ( $3.6\pm 2.8\%$  for nvPM number and  $5.8\pm 4.6\%$  for nvPM mass). It should be noted that the  
 428 percentage difference equations given in **Figure 7** are only valid for the investigated APU and  
 429 operating conditions with the selected fuels and may not be applicable to other engines or fuels.  
 430 However, this analysis method can be applied to emissions data from other engine types to compare  
 431 the reduction in nvPM emissions for sustainable aviation fuels and blends.



433 **Figure 7: Percent difference in EEP-corrected nvPM number- (a) and nvPM mass- (b) -based**  
 434 **emission indices (relative to 14.33% fuel hydrogen content data) as a function of fuel hydrogen**  
 435 **content (i.e. %H<sub>content</sub>) combining data for the three APU operating conditions from the two ITAKA**  
 436 **test campaigns**

#### 437 **4. Conclusion**

438 The nvPM number and mass emissions and particle size distributions from a GTCP85 aircraft APU  
 439 burning blends of two sustainable fuels (UCO-HEFA and Camelina-HEFA) blended with different  
 440 batches of conventional Jet A-1 fuel were measured at different operating conditions during two  
 441 separate test campaigns, ITAKA 1 and ITAKA 2. The North American mobile reference system was used  
 442 during ITAKA 1 and the European mobile reference system was used during ITAKA 2.

443 The results of this work have confirmed that the fuel hydrogen content is a well-suited parameter to  
 444 correlate EEP nvPM emissions reductions, within the current measurement uncertainty, using

445 standardised sampling and measurement reference systems. Increasing the fuel hydrogen content  
446 was shown to significantly reduce nvPM EIs at the measurement location and at EEP. The absolute  
447 nvPM number and mass emissions were consistently higher during ITAKA 2 which can be attributed  
448 to a number of factors including emission source variability (ambient conditions, exhaust stream  
449 spatial inhomogeneity, engine wear, etc) and measurement uncertainty (calibration tolerances,  
450 dilution factor measurement, etc) between the two ITAKA test campaigns. Given the two investigated  
451 alternative fuels have relatively similar fuel compositions and the common APU source, the findings  
452 of this study should be further validated using fuels of significantly different chemical composition and  
453 physical properties in different engine types to validate the overall reduction in nvPM emissions and  
454 the potential improvement to local air quality that the adoption of sustainable aviation fuels may offer.

455 The results of this work also highlight that particle loss correction is critical to accurately quantifying  
456 EEP nvPM emissions and reduction, which can be used to assess the impact on local air quality. A  
457 standard procedure to correct for particle loss in a standard sampling and measurement system using  
458 nvPM number and mass emissions data is currently available [26,44], however it assumes a GMD and  
459 GSD, and it does not include a measurement of particle size distribution to assess losses as presented  
460 in this work. Further work would also be required to quantify the impact of ambient condition, engine  
461 variability, sampling representativeness, and system-to-system measurement variability on nvPM  
462 measurement to better explain the systematic differences in the measured nvPM emissions between  
463 ITAKA 1 and ITAKA 2 which would enable better quantification of the impact of fuel hydrogen content.

## 464 **Acknowledgments**

465 This work was partly supported by the European Union's Seventh Framework Programme under Grant  
466 Agreement 308807 ITAKA (Initiative Towards sustAinable Kerosene for Aviation), an EASA framework  
467 contract concerned with Support on technical issues associated with aviation emissions  
468 (EASA.2015.FC21), with support for the preparation of this paper funded by the EU Horizon 2020  
469 AVIATOR project (Grant agreement ID: 814801), and the FLEXIS project (Welsh European Funding

470 Office Grant 80835). Any opinions, findings, and conclusions or recommendations expressed in this  
471 paper are those of the authors and do not necessarily reflect the views of the sponsors.

## 472 References

- 473 [1] Advisory Council for Aviation Research and Innovation in Europe (ACARE). Strategic Research &  
474 Innovation Agenda - 2017 Update Volume 1 2017.  
475 [https://www.acare4europe.org/sites/acare4europe.org/files/document/ACARE-Strategic-](https://www.acare4europe.org/sites/acare4europe.org/files/document/ACARE-Strategic-Research-Innovation-Volume-1.pdf)  
476 [Research-Innovation-Volume-1.pdf](https://www.acare4europe.org/sites/acare4europe.org/files/document/ACARE-Strategic-Research-Innovation-Volume-1.pdf).
- 477 [2] ACI. Annual World Airport Traffic Report (WATR) 2018. [https://aci.aero/wp-](https://aci.aero/wp-content/uploads/2018/11/WATR_WATF_Infographic_Web.pdf)  
478 [content/uploads/2018/11/WATR\\_WATF\\_Infographic\\_Web.pdf](https://aci.aero/wp-content/uploads/2018/11/WATR_WATF_Infographic_Web.pdf).
- 479 [3] Becken S, Shuker J. A framework to help destinations manage carbon risk from aviation  
480 emissions. *Tour Manag* 2019;71:294–304. <https://doi.org/10.1016/j.tourman.2018.10.023>.
- 481 [4] Carbon Offsetting and Reduction Scheme for International Aviation (CORSA) n.d.  
482 <https://www.icao.int/environmental-protection/CORSIA/Pages/default.aspx> (accessed July 2,  
483 2020).
- 484 [5] Masiol M, Harrison RM. Aircraft engine exhaust emissions and other airport-related  
485 contributions to ambient air pollution: A review. *Atmos Environ* 2014;95:409–55.  
486 <https://doi.org/10.1016/j.atmosenv.2014.05.070>.
- 487 [6] Lobo P, Hagen DE, Whitefield PD, Raper D. PM emissions measurements of in-service  
488 commercial aircraft engines during the Delta-Atlanta Hartsfield Study. *Atmos Environ*  
489 2015;104:237–45. <https://doi.org/10.1016/j.atmosenv.2015.01.020>.
- 490 [7] Boies AM, Stettler MEJ, Swanson JJ, Johnson TJ, Olfert JS, Johnson M, et al. Particle Emission  
491 Characteristics of a Gas Turbine with a Double Annular Combustor. *Aerosol Sci Technol*  
492 2015;49:842–55. <https://doi.org/10.1080/02786826.2015.1078452>.
- 493 [8] Delhay D, Ouf F-X, Ferry D, Ortega IK, Penanhoat O, Peillon S, et al. The MERMOSE project:  
494 Characterization of particulate matter emissions of a commercial aircraft engine. *J Aerosol Sci*  
495 2017;105:48–63. <https://doi.org/10.1016/j.jaerosci.2016.11.018>.
- 496 [9] Shirmohammadi F, Sowlat MH, Hasheminassab S, Saffari A, Ban-Weiss G, Sioutas C. Emission  
497 rates of particle number, mass and black carbon by the Los Angeles International Airport (LAX)  
498 and its impact on air quality in Los Angeles. *Atmos Environ* 2017;151:82–93.  
499 <https://doi.org/10.1016/j.atmosenv.2016.12.005>.
- 500 [10] Keuken MP, Moerman M, Zandveld P, Henzing JS, Hoek G. Total and size-resolved particle  
501 number and black carbon concentrations in urban areas near Schiphol airport (the Netherlands).  
502 *Atmos Environ* 2015;104:132–42. <https://doi.org/10.1016/j.atmosenv.2015.01.015>.
- 503 [11] Jonsdottir HR, Delaval M, Leni Z, Keller A, Brem BT, Siegerist F, et al. Non-volatile particle  
504 emissions from aircraft turbine engines at ground-idle induce oxidative stress in bronchial cells.  
505 *Commun Biol* 2019;2:90. <https://doi.org/10.1038/s42003-019-0332-7>.
- 506 [12] Lee DS, Fahey DW, Forster PM, Newton PJ, Wit RCN, Lim LL, et al. Aviation and global climate  
507 change in the 21st century. *Atmos Environ* 2009;43:3520–37.  
508 <https://doi.org/10.1016/j.atmosenv.2009.04.024>.
- 509 [13] Kärcher B. The importance of contrail ice formation for mitigating the climate impact of aviation.  
510 *J Geophys Res Atmospheres* 2016;121:3497–505. <https://doi.org/10.1002/2015JD024696>.
- 511 [14] Burkhardt U, Bock L, Bier A. Mitigating the contrail cirrus climate impact by reducing aircraft soot  
512 number emissions. *Npj Clim Atmospheric Sci* 2018;1:37. [https://doi.org/10.1038/s41612-018-](https://doi.org/10.1038/s41612-018-0046-4)  
513 [0046-4](https://doi.org/10.1038/s41612-018-0046-4).
- 514 [15] ICAO. Annex 16 - Environmental Protection Volume 2 - Aircraft Engine Emissions. 2017.

- 515 [16] SAE international. ARP 6320 - Procedure for the Continuous Sampling and Measurement of Non-  
516 Volatile Particulate Matter Emissions from Aircraft Turbine Engines 2018.  
517 <https://doi.org/10.4271/ARP6320>.
- 518 [17] Petzold A, Marsh R. SAMPLE I-Studying, sAmpling and Measuring of Particulate Matter 2009.  
519 <https://www.easa.europa.eu/document-library/research-reports/easa2008op13>.
- 520 [18] Marsh R, Crayford A, Petzold A, Johnson M. SAMPLE II-Studying, sAmpling and Measuring of  
521 Particulate Matter II 2011. [https://www.easa.europa.eu/document-library/research-](https://www.easa.europa.eu/document-library/research-reports/easa2009op18)  
522 [reports/easa2009op18](https://www.easa.europa.eu/document-library/research-reports/easa2009op18).
- 523 [19] Crayford A, Johnson M. SAMPLE III SC.01- Studying, sAmpling and Measuring of aircraft  
524 Particulate Emission 2011. [https://www.easa.europa.eu/document-library/research-](https://www.easa.europa.eu/document-library/research-reports/easa2010fc10-sc01)  
525 [reports/easa2010fc10-sc01](https://www.easa.europa.eu/document-library/research-reports/easa2010fc10-sc01).
- 526 [20] Crayford A, Johnson M. SAMPLE III SC.02 - Studying, sAmpling and Measuring of aircraft  
527 Particulate Emission 2012. [https://www.easa.europa.eu/document-library/research-](https://www.easa.europa.eu/document-library/research-reports/easa2010fc10-sc02)  
528 [reports/easa2010fc10-sc02](https://www.easa.europa.eu/document-library/research-reports/easa2010fc10-sc02).
- 529 [21] Crayford A, Johnson M. SAMPLE III SC.03- Studying, sAmpling and Measuring of aircraft  
530 Particulate Emission 2013. [https://www.easa.europa.eu/document-library/research-](https://www.easa.europa.eu/document-library/research-reports/easa2010fc10-sc03)  
531 [reports/easa2010fc10-sc03](https://www.easa.europa.eu/document-library/research-reports/easa2010fc10-sc03).
- 532 [22] Crayford A, Johnson M, Sevcenco Y, Williams P. SAMPLE III SC.05 - Studying, sAmpling and  
533 Measuring of aircraft Particulate Emission 2014. [https://www.easa.europa.eu/document-](https://www.easa.europa.eu/document-library/research-reports/easa2010fc10-sc05)  
534 [library/research-reports/easa2010fc10-sc05](https://www.easa.europa.eu/document-library/research-reports/easa2010fc10-sc05).
- 535 [23] Petzold A, Marsh R, Johnson M, Miller M, Sevcenco Y, Delhay D, et al. Evaluation of Methods  
536 for Measuring Particulate Matter Emissions from Gas Turbines. *Environ Sci Technol*  
537 2011;45:3562–8. <https://doi.org/10.1021/es103969v>.
- 538 [24] Lobo P, Durdina L, Smallwood GJ, Rindlisbacher T, Siegerist F, Black EA, et al. Measurement of  
539 Aircraft Engine Non-Volatile PM Emissions: Results of the Aviation-Particle Regulatory  
540 Instrumentation Demonstration Experiment (A-PRIDE) 4 Campaign. *Aerosol Sci Technol*  
541 2015;49:472–84. <https://doi.org/10.1080/02786826.2015.1047012>.
- 542 [25] Lobo P, Durdina L, Brem BT, Crayford AP, Johnson MP, Smallwood GJ, et al. Comparison of  
543 standardized sampling and measurement reference systems for aircraft engine non-volatile  
544 particulate matter emissions. *J Aerosol Sci* 2020:105557.  
545 <https://doi.org/10.1016/j.jaerosci.2020.105557>.
- 546 [26] SAE international. ARP 6481- Procedure for the Calculation of Sampling Line Penetration  
547 Functions and Line Loss Correction Factors 2019. <https://doi.org/10.4271/ARP6481>.
- 548 [27] Hileman JI, Stratton RW, Donohoo PE. Energy Content and Alternative Jet Fuel Viability. *J Propuls*  
549 *Power* 2010;26:1184–96. <https://doi.org/10.2514/1.46232>.
- 550 [28] Petroleum Quality Information System 2013 Annual Report. DEFENSE LOGISTICS AGENCY FORT  
551 BELVOIR VA; 2013.
- 552 [29] Beyersdorf AJ, Timko MT, Ziemba LD, Bulzan D, Corporan E, Herndon SC, et al. Reductions in  
553 aircraft particulate emissions due to the use of Fischer–Tropsch fuels. *Atmospheric Chem Phys*  
554 2014;14:11–23. <https://doi.org/10.5194/acp-14-11-2014>.
- 555 [30] Lobo P, Condevaux J, Yu Z, Kuhlmann J, Hagen DE, Miake-Lye RC, et al. Demonstration of a  
556 Regulatory Method for Aircraft Engine Nonvolatile PM Emissions Measurements with  
557 Conventional and Isoparaffinic Kerosene fuels. *Energy Fuels* 2016;30:7770–7.  
558 <https://doi.org/10.1021/acs.energyfuels.6b01581>.
- 559 [31] Lobo P, Rye L, Williams PI, Christie S, Uryga-Bugajska I, Wilson CW, et al. Impact of Alternative  
560 Fuels on Emissions Characteristics of a Gas Turbine Engine – Part 1: Gaseous and Particulate  
561 Matter Emissions. *Environ Sci Technol* 2012;46:10805–11. <https://doi.org/10.1021/es301898u>.
- 562 [32] Schripp T, Herrmann F, Oßwald P, Köhler M, Zschocke A, Weigelt D, et al. Particle emissions of  
563 two unblended alternative jet fuels in a full scale jet engine. *Fuel* 2019;256:115903.  
564 <https://doi.org/10.1016/j.fuel.2019.115903>.

- 565 [33] Rojo C, Vancassel X, Mirabel P, Ponche J-L, Garnier F. Impact of alternative jet fuels on aircraft-  
566 induced aerosols. *Fuel* 2015;144:335–41. <https://doi.org/10.1016/j.fuel.2014.12.021>.
- 567 [34] Yim SHL, Stettler MEJ, Barrett SRH. Air quality and public health impacts of UK airports. Part II:  
568 Impacts and policy assessment. *Atmos Environ* 2013;67:184–92.  
569 <https://doi.org/10.1016/j.atmosenv.2012.10.017>.
- 570 [35] Lobo P, Hagen DE, Whitefield PD. Comparison of PM Emissions from a Commercial Jet Engine  
571 Burning Conventional, Biomass, and Fischer–Tropsch Fuels. *Environ Sci Technol* 2011;45:10744–  
572 9. <https://doi.org/10.1021/es201902e>.
- 573 [36] Lobo P, Christie S, Khandelwal B, Blakey S, Raper D. Evaluation of Non-Volatile PM Emissions  
574 Characteristics of an Aircraft Auxiliary Power Unit with Varying Alternative Jet Fuel Blend Ratios.  
575 *Energy Fuels* 2015;29:151016011415009. <https://doi.org/10.1021/acs.energyfuels.5b01758>.
- 576 [37] Chiaramonti D, Prussi M, Buffi M, Tacconi D. Sustainable bio kerosene: Process routes and  
577 industrial demonstration activities in aviation biofuels. *Appl Energy* 2014;136:767–74.  
578 <https://doi.org/10.1016/j.apenergy.2014.08.065>.
- 579 [38] Christie S, Lobo P, Lee D, Raper D. Gas Turbine Engine Nonvolatile Particulate Matter Mass  
580 Emissions: Correlation with Smoke Number for Conventional and Alternative Fuel Blends.  
581 *Environ Sci Technol* 2017;51:988–96. <https://doi.org/10.1021/acs.est.6b03766>.
- 582 [39] Lobo P, Hagen DE, Whitefield PD, Alofs DJ. Physical Characterization of Aerosol Emissions from  
583 a Commercial Gas Turbine Engine. *J Propuls Power* 2007;23:919–29.  
584 <https://doi.org/10.2514/1.26772>.
- 585 [40] Durdina L, Brem BT, Abegglen M, Lobo P, Rindlisbacher T, Thomson KA, et al. Determination of  
586 PM mass emissions from an aircraft turbine engine using particle effective density. *Atmos*  
587 *Environ* 2014;99:500–7. <https://doi.org/10.1016/j.atmosenv.2014.10.018>.
- 588 [41] Hagen DE, Lobo P, Whitefield PD, Trueblood MB, Alofs DJ, Schmid O. Performance Evaluation of  
589 a Fast Mobility-Based Particle Spectrometer for Aircraft Exhaust. *J Propuls Power* 2009;25:628–  
590 34. <https://doi.org/10.2514/1.37654>.
- 591 [42] Durand EF, Crayford AP, Johnson M. Experimental validation of thermophoretic and bend  
592 nanoparticle loss for a regulatory prescribed aircraft nvPM sampling system. *Aerosol Sci Technol*  
593 2020;0:1–15. <https://doi.org/10.1080/02786826.2020.1756212>.
- 594 [43] Altaher MA, Li H, Williams P, Johnson M, Blakey S. Determination of Particle Penetration Factors  
595 in a Particle Transfer Line for Aero Gas Turbine Engine Exhaust Particle Measurement  
596 2014:V04AT04A028. <https://doi.org/10.1115/GT2014-25440>.
- 597 [44] SAE international. AIR 6504 - Procedure for the Calculation of Sampling System Penetration  
598 Functions and System Loss Correction Factors 2017. <https://doi.org/10.4271/AIR6504>.
- 599 [45] Brem BT, Durdina L, Siegerist F, Beyerle P, Bruderer K, Rindlisbacher T, et al. Effects of Fuel  
600 Aromatic Content on Nonvolatile Particulate Emissions of an In-Production Aircraft Gas Turbine.  
601 *Environ Sci Technol* 2015;49:13149–57. <https://doi.org/10.1021/acs.est.5b04167>.
- 602